LEGIBILITY NOTICE

A major purpose of the Technical Information Center is to provide the broadest dissemination possible of information contained in DOE's Research and Development Reports to business, industry, the academic community, and federal, state and local governments.

Although a small portion of this report is not reproducible, it is being made available to expedite the availability of information on the research discussed herein.

LA-UR -89-2768

Los Alamos National Laboratory is operated by the University of California for the United States Department of Energy under contract W-7405-ENG-36

LA-UR--89-2768

DE89 016367

TITLE A NUMERICAL LABORATORY FOR GRANULAR SOLIDS

AUTHOR(S) B. C. Trent, EES-5
L. G. Margolin, LANL

SUBMITTED TO First U. S. Conf. on Discrete Element Methods,
Golden, CO
October 19-20, 1989

DISCLAIMER

Los Alamos Los Alamos National Laboratory
Los Alamos, New Mexico 87545

A NUMERICAL LABORATORY FOR GRANULAR SOLIDS

B.C. Trent
Los Alamos National Laboratory
Los Alamos, NM 87545

L.G. Margolin
Lawrence Livermore National Laboratory
Livermore, CA 94550

INTRODUCTION

The behavior of cemented granular material is complex and difficult to characterize. Physical tests on laboratory-size specimens are time consuming and often inconclusive, due to the variable nature of the bulk material. Samples of weakly-cemented material are difficult to prepare and the results of testing are not always reproducible. Nevertheless, constitutive models have been formulated, generally relying on plasticity theory, so that large scale calculations of boundary value problems may be performed. These phenomenological material models neglect the underlying physical processes that cause the observed behavior and concentrate on curve-fitting or "knob-twiddling" techniques to provide reasonable macroscopic response.

As an alternate approach, we have used the distinct element method to construct numerical samples of cemented granular material. The model allows us to verify which are the important microphysical processes determining material behavior. We can do parameter studies, continuously varying the material properties of the bonding material and the topology of the bonds themselves, to see how the macroscopic properties depend upon the microscopic structure. The first step in this process has been to verify that the numerical model accurately reproduces the qualitative behavior of real granular materials. Our longer term goal is to develop an analytic model based on the limited set of processes in the distinct element computer program that captures the most important features of real granular materials.

We illustrate our program with two types of calculations. The first series consists of measuring the macroscopic p-wave and the s-wave speeds of the numerical sample, and using them to infer elastic properties of the bulk material. A simple dimensional analysis shows that the macroscopic elastic moduli must be directly proportional to the moduli of the bonding material.

This relation is verified. We also investigate how the number and size of the bonds influence bulk response.

In the second series, we look at crack growth in granular materials. The Griffith theory of crack growth assumes an ideally flat crack. In granular materials and in our simulations, the crack is formed when many consecutive bonds in the material are broken. Such a crack is not flat. Nevertheless, we show that the classic relation between crack size and the critical stress for the onset of growth remains valid.

INFLUENCE OF BOND CHARACTERISTICS ON MACROSCOPIC WAVE SPEEDS

The distinct element model assumes a system of spherical rigid particles that are constrained to move in only two dimensions. Elastic bonds are placed between certain pairs of particles. Within each bond is a Griffith crack, oriented perpendicular to the line joining the particle centers. The geometry is described by the three dimensionless parameters, i.e. α, β, and δ, that are illustrated in Fig. 1. α is the total width of the bond, β is the width of the Griffith crack, and δ is the length of the bond. Each of the parameters is nondimensionalized by the particle radius, R. Under load, the particles are displaced relative to each other. Restoring forces and torques are applied to each bonded particle pair by analytic equations developed for the three independent modes of deformation: simple tension/compression (i.e., the bonded particles moving toward or away from each other); rolling torsion (i.e., one particle rotating clockwise and the other counterclockwise); and shearing torsion (both particles rotating in the same angular direction). The details of this formulation are given by Trent (1987,1988,1989). For example, the form of the restoring forces in simple tension is:

$$(1)\quad \frac{F/\Delta u}{E} = -w + \frac{a}{\sqrt{a^2 - 1}} \arccos\left(\frac{a\cos(w) - 1}{a - \cos(w)} \right) \qquad \begin{matrix} w=\arcsin(\alpha) \\ w=\arcsin(\beta) \end{matrix}, \quad (a=1+\delta).$$

Here F is the restoring force, Δu is the incremental stretching, and E is the elastic modulus of the bonding material.

The sample is shown in Fig. 2. There are 270 particles, each with a radius of 1 mm, and 397 bonds. The material is formed by allowing particles

to settle under gravity and then bonding all particles whose centers are closer han 0.25 mm. None of the particles are touching so there are no direct particle-particle contacts, unlike most distinct element simulations. In the wave propagation analyses presented in this section, no crack growth is allowed so that the parameter $\bar{\beta}$ remains constant during the simulation. The value of $\bar{\beta}$ in case 4 differs from the other cases. In all the simulations, the bond width ($2\bar{\alpha}R$) is 1 mm so that $\bar{\alpha}$=0.5.

Boundary conditions are prescribed by specifying the velocities of the lower twenty particles. For generating the tensile waves, these particles are given a constant downward velocity of 10 m/s for a short time. Their velocity is then set to zero and the resulting ringing of the sample recorded. Average vertical velocities for particles in each of the six shaded regions in Fig. 2 were calculated and plotted as functions of time. Figure 3 shows the p-wave response for the baseline case. Note that the amplitude does not decrease from cycle to cycle so the response is undamped.

Twelve numerical experiments were performed, representing six different materials. A shear wave was generated by applying a horizontal boundary condition to the twenty lower fixed particles. Similarly, the horizontal velocities for the particles in the shaded regions were averaged and plotted and functions of time. Figure 4 shows this response for the baseline case. The p-wave and s-wave velocities were measured by calculating the average time required for waves to travel through the sample. For example, Fig. 3 shows seven complete cycles in 303 usec. Since the length of the sample is 32 mm, a complete cycle must travel 64 mm, so c_ℓ= (7 x 64e-3 m) / (303e-6 s) or 1480 m/s. This value is typical of alluvium, a cemented granular material.

Returning to Eq. 1, we note that the stiffest bonds are those with small bond lengths, with small initial cracks and with large bond widths. In general, the individual forces between bonded particles depend on the geometric parameters ($\bar{\alpha}$, $\bar{\beta}$, $\bar{\delta}$) and on the elastic properties of the bond (E). However, E is the only parameter in the problem with the dimensions of a modulus, and so based on dimensional analysis, we would predict that the effective modulus of the granular material must scale directly with the elastic modulus of the bond. The results in Table 1 verify this conclusion. The wave speed in a homogeneous, isotropic solid depends on the square root of the modulus. Thus in comparing tests 1 and 2, where E drops by a factor

of 2, we would expect the p-wave speed to drop by the square root of 2. The numerical ratio is actually 1.41. Similarly, the s-wave speed drops by the factor 1.36.

When the maximum distance used to determine which particles are bonded is increased from 0.25 mm to 0.5 mm in tests 3 and 4, the number of bonds in the problem increases from 397 to 480. These additional bonds are much less stiff than bonds with smaller separation. Nevertheless, adding only 21% more of these bonds has the same effect as doubling the elastic modulus - compare tests 1 and 2 and 3. Clearly, the topology of the bonds plays a major role in macroscopic response. We are currently building an analytic model to quantify these numerical results, which will lead to a constitutive law for use in a continuum code.

In test 4 the initial crack size was increased (for every bond) from 2.5% to 20% of the bond width. This has the expected effect of decreasing the wave speeds. In a real granular material, each bond may have a different thickness and therefore a different stiffness. This complexity is not included in the present analyses, but the effect could be modeled by allowing the initial crack within each bond to be selected from some distribution.

The effect of Poisson's ratio in the bonding material was also examined. Cases 1 to 4 assumed a value of 0.18 but case 5 uses 0.05 and case 6 uses 0.45. Very little difference in the macroscopic response is observed even though the shear modulus of the bond material varies by 38%. We conclude that the macroscopic Poisson's ratio depends most strongly on the bond topology. This is not too surprising since the shear modulus of the bonds only affects the restoring force in the shearing torsion mode.

The results of these 12 numerical experiments may be combined by calculating a macroscopic modulus and Poisson's ratio, expressed in terms of the wave speeds:

$$(2) \qquad \nu = 1/2 \left[(c_l^2 - 2\, c_s^2) / (c_l^2 - c_s^2) \right]$$

$$(3) \qquad E/\rho = c_s^2 \left[2 + (c_l^2 - 2\, c_s^2) / (c_l^2 - c_s^2) \right]$$

where ν is Poisson's ratio, E is the elastic modulus and ρ is the bulk material density. Table 1 shows these macroscopic quantities for each of the six different cases.

Table 1. Macroscopic Poisson's Ratio and Modulus for Cases 1 to 6

Test	c_l (m/s)	c_s (m/s)	ν	E/ρ $(m/s)^2$	Description
1	1480	830	0.271	1.75e6	Baseline
2	1050	610	0.245	0.93e6	1/2 E
3	1430	830	0.246	1.72e6	1/2 E, 83 more bonds
4	1160	650	0.271	1.07e6	1/2 E, 83 more bonds, 20% damaged
5	1490	850	0.259	1.82e6	Baseline, but ν of bonds=0.05
6	1440	810	0.269	1.66e6	Baseline, but ν of bonds=0.45

This table shows that a reduction in the elastic modulus of the bonds has roughly the effect of reducing the macroscopic modulus by the same factor. It is of interest to note that the macroscopic Poisson's ratio only varied from 0.245 to 0.271, or ten percent, for all six cases. Nearly all the mass of the system is contained in the particles, since the cross-section of the bonds is relatively small. A density of 2650 kg/m^3 was used, representing the density of quartz. The porosity of the sample in Fig. 2 is 36.9%, so the bulk density is roughly 1670 kg/m^3. Using this value, the macroscopic elastic modulus is 2920 MPa for the baseline case, or only 14.6% of the value of the individual bonds. This percentage would be much higher if the sample were more closely packed and more completely bonded.

THE EFFECT OF INITIAL FLAW SIZE ON MACROSCOPIC TENSILE FAILURE

The Griffith theory (Griffith, 1920) predicts the onset of growth of an ideal crack in an elastic continuum (Margolin, 1984a). An important prediction of this theory is that the threshold stress for crack growth is proportional to the reciprocal of the square root of crack length. Several researchers have built constitutive models for geologic materials in which fracture is described in terms of the growth of a distribution of preexisting cracks whose number and size are assumed to be known as a material property (Seaman et al 1976, Margolin 1984b). However the assumptions of the Griffith theory are not well-realized in granular materials, which are

inhomogeneous on a length scale comparable to the crack size. In particular, cracks in granular materials are not necessarily flat.

The purpose of the calculations in this section is to investigate the validity of Griffith theory in granular materials. Recall that each bond has within it a small ideal Griffith crack. The idea in this section is to embed a macroscopic crack into the numerical sample by severing the bonds between several sets of adjacent particles. Then we subject the material to a tensile stress at the boundaries that strains the crack. As in the Griffith theory, stress concentrations appear at the first set of unbroken bonds at the ends of the crack, which will cause the microscopic crack within those bonds to grow. When this microscopic crack grows to be the width of the bond, the bond is broken and the macroscopic crack is said to have grown. In the numerical experiments, we build up the boundary stress slowly to mimic a quasistatic test, and we record the stress level when the first new bond breaks. It is important to use enough particles in the simulation to assure that the boundaries have negligible effect.

All the simulations in this section are done with the regular array of particles shown in Fig. 5. In the first, benchmark set, the initial macroscopic crack is formed by severing bonds all in the same plane. From these calculations, we conclude that is necessary for the initial crack to be made of at least 5 or 6 bonds for the Griffith theory to apply. Physically, a lesser number corresponds to the breakdown of the continuum approximation. Furthermore, in a numerical sense, it is not clear how to measure the crack length itself when it is on the same order as the bond. The results are shown in Fig. 6. As the initial crack length increases, the slope of the curve approaches -0.5, the theoretical value derived by Griffith, shown by the dashed line.

In the second set of calculations, we made the initial macroscopic crack irregular by severing the bonds in several different though parallel planes. The initial conditions are sketched in Fig. 7. Although the cracks span the same total length as the corresponding cracks in the first set, the bonds between the particles at the ends of the individual planes are not broken. The results of these calculations show a higher threshold for fracture, which we interpret as modeling the growth of several smaller, but unconnected initial cracks. Note in Fig. 6 that very little decrease in strength is realized as the (total) initial crack length increases.

In the third set of calculations we modified the preceding set by also severing the bonds between the end particles of the individual planes. The crack is more continuous than in the second set of calculations. There are also more broken bonds per unit length than in either the first or second set. The interesting result is that when the initial crack is long enough (again, 5 or 6 bonds) the results lie almost on top of the results of the first set. The conclusion is that we can use the Griffith theory to describe the onset of growth of an irregular (as opposed to flat) crack so long as the initial crack encompasses at least 9 bonds.

SUMMARY

The distinct element method has been used to perform a number of numerical experiments, analogous to physical tests routinely carried out for real geologic materials. The ability to prescribe exactly the material properties and the boundary conditions allow us to study in detail the influence of microscopic structure on macroscopic response. These macroscopic quantities are usually the only data obtained in physical experiments. We are now in a position to formulate a general constitutive model, based on physical mechanisms and appropriate for use in a continuum code.

ACKNOWLEDGMENT

This work was performed under the auspices of the U.S. Department of Energy.

REFERENCES

Griffith, A.A,"Phenomena of Rupture and Flow in Solids," Phil. Trans. Royal Soc. A. 221, 1921.

Margolin, L.G., 1984a, "Generalized Griffith Criteria for Crack Propagation," Engineering Fracture Mechanics, 19, pp. 539-543.

Margolin, L.G., 1984b, "Microphysical Models for Inelastic Response," International Journal of Engineering Science, 22.

Seama L., D.R. Curran, and D.A. Shockey, 1976, "Computational Models for Ducti and Brittle Fracture," J. Appl. Phys., 47, pp. 4814-4826.

Trent, B.C., 1987, "The Effect of Micro-Structure on the Macroscopic Behavior of Cemented Granular Material," Ph.D. Thesis, University of Minnesota, Minneapolis, MN.

Trent, B.C., 1988, "Microstructural Effects in Static and Dynamic Numerical Experiments," Proceedings of the 29th U.S. Symposium on Rock Mechanics, Minneapolis, MN, pp 395-402.

Trent B.C., 1989, "Numerical Simulation of Wave Propagation Through Cemented Granular Material," Proceedings of the A.S.M.E. International Symposium on Wave Propagation in Granular Media, San Francisco, CA.

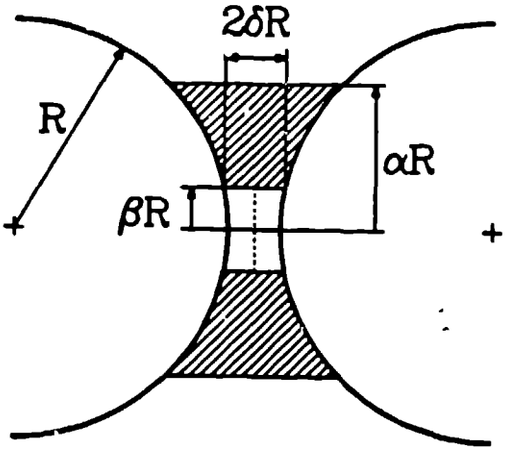

Fig. 1 Elastic bonding material defined by three dimensionless coefficients.

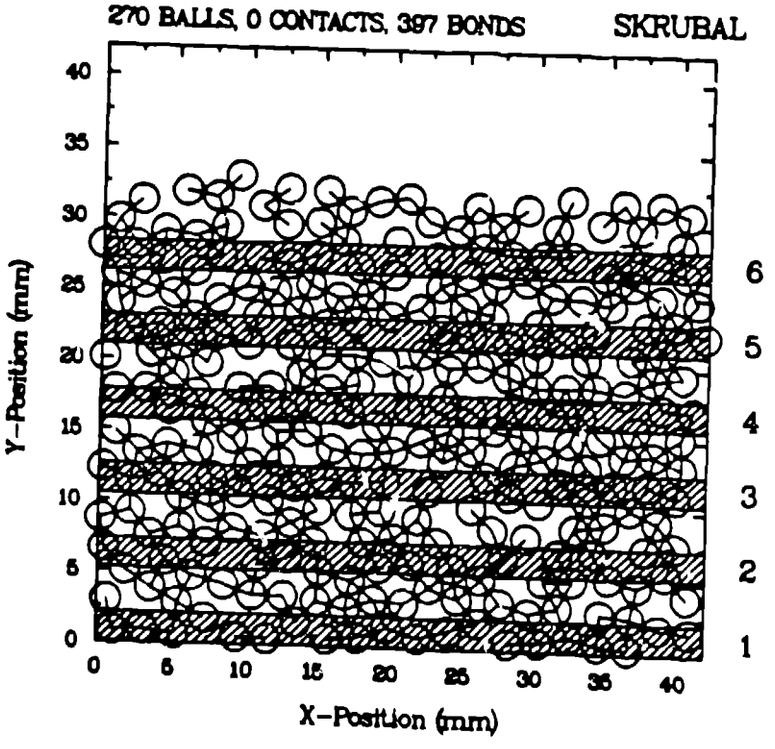

Fig. 2 Sample of 270 particles and 397 bonds (represented by the straight lines). The shaded areas are regions where particle velocities are averaged. The velocities are prescribed for the lower 20 particles and the top surface is free.

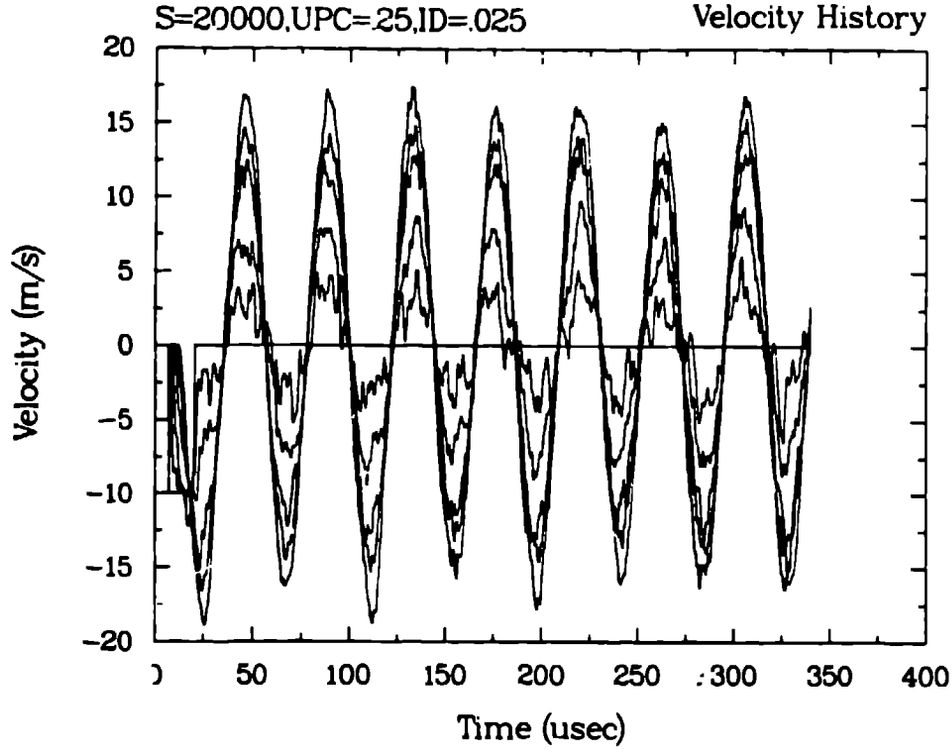

Fig. 3 Time histories of vertical velocities in the shaded regions shown in Fig. 2 due to vertical loading of the lower boundary (test 1). The p-wave velocity is 1480 m/s.

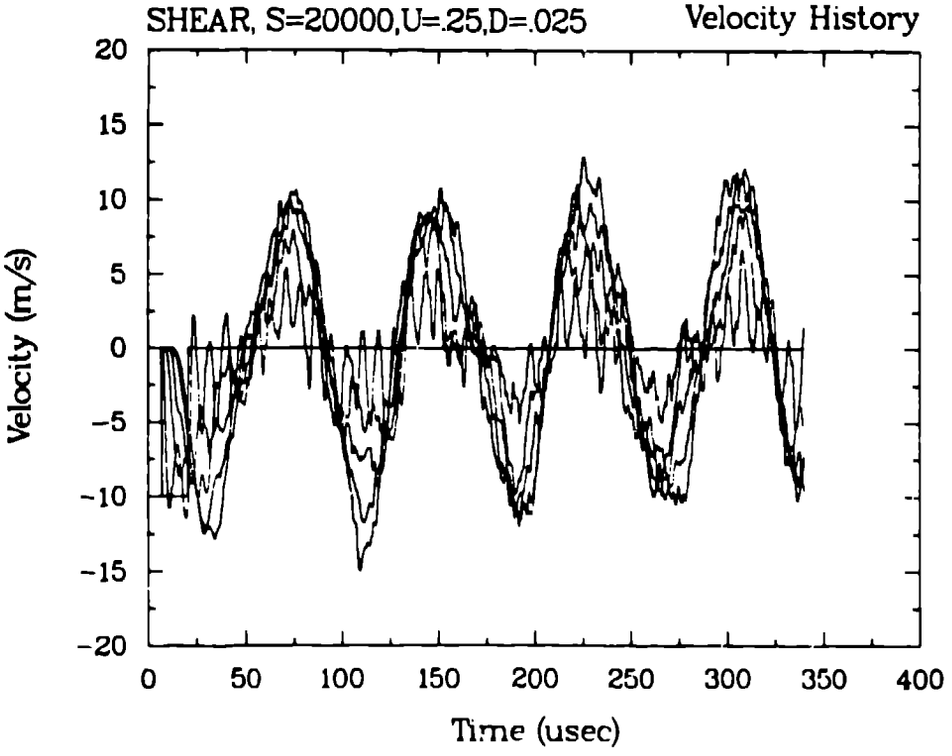

Fig. 4 Time histories of horizontal velocities in the shaded regions shown in Fig. 2 due to horizontal loading of the lower boundary (test 1). The s-wave velocity is 830 m/s.

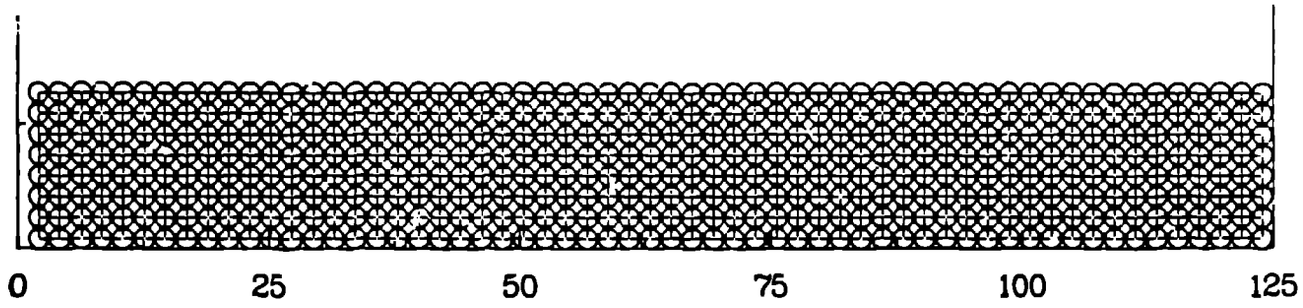

Fig. 5 Particle distribution for the quasistatic tensile tests. There are 8 x 59 or 472 particles and 877 bonds. The lower layer of particles is fixed and the upper layer moves slowly upward until one bond breaks, leading to rupture of sample.

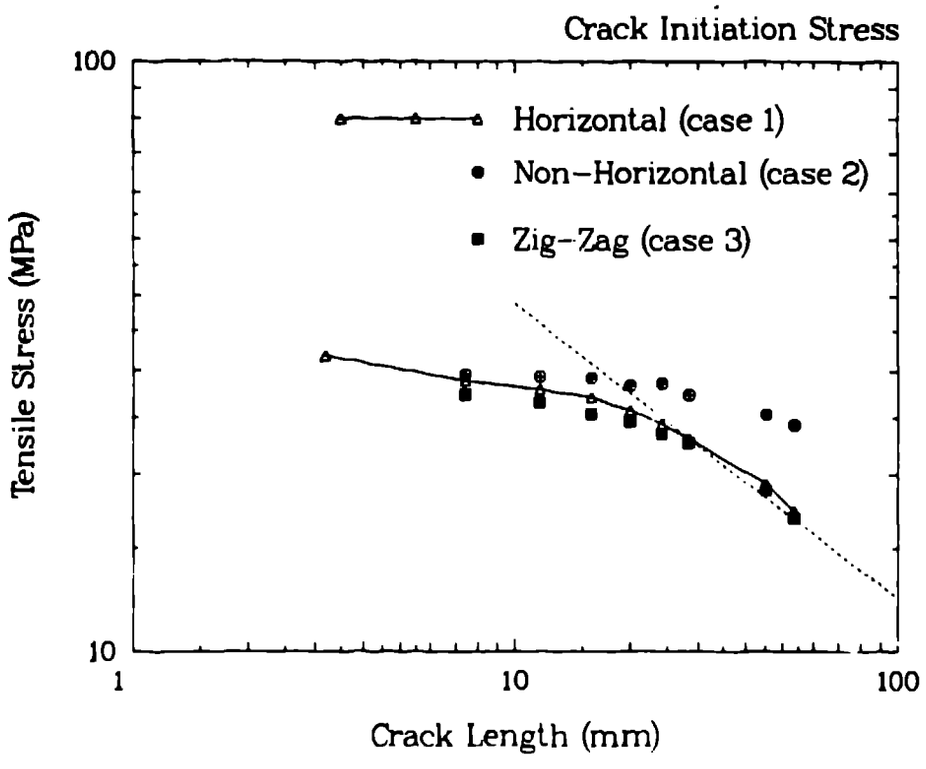

Fig. 6 Ultimate tensile strength vs. crack length for the three cases. The slope of the curve for tests with at least 9 initially broken bonds is nearly 1/2, the value derived by Griffith theory.

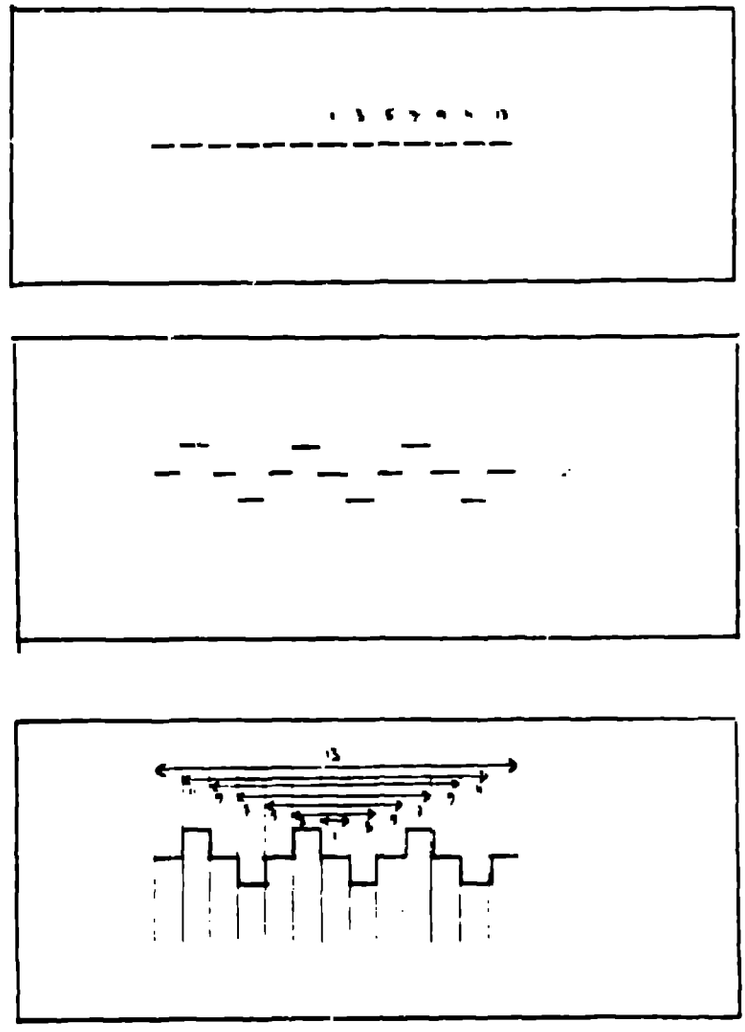

Fig. 7 Schematic diagram of the initial crack distribution for each of the three cases.